IJISET - International Journal of Innovative Science, Engineering & Technology, Vol. 4 Issue 10, October 2017
ISSN (Online) 2348 – 7968 | Impact Factor (2016) – 5.264
www.ijiset.com

Prediction of radiative heat transfer in a combustion chamber

SAGOUONG Jean Michel [1,2,3,*], KAMDEM TAGNE Hervé Thierry [1] , TCHUEN Ghislain [2,3]

[1] Laboratory of Mechanics and Physical Systems Modeling (L2MSP), Department of Physics, University of Dschang, POBox 67 Dschang, Cameroon.

[2] Department of Energetic Environment and Thermal engineering, University Institute of Technology of Bandjoun, West, Bandjoun, Cameroun

[3] Laboratory of Engineering of Industrial Systems and Environment (LISIE), UIT-FV Bandjoun, University of DSchang, POBox134 Bandjoun, Cameroon

Abstract

The method used to predict radiative heat transfer in combustion chambers in this work is the Patankar's method. Here, the two-dimensional moment of intensity partial differential equations are combined to yield a single second-order partial differential equation for P-1approximation. The P-1 approximation results are compared with numerical Hottel zone results. Studies show that the P-1 approximation can be used to predict emissive power distribution.

Keywords: *Radiation, Heat transfer, Combustion chamber, Spherical harmonic, emissive power.*

1. Introduction

The study of radiative heat transfer radiating media has become increasingly important in such diverse fields as cryogenics, ablative protection, glass manufacture, and energy conservation. It is the dominant mode of heat transfer in applications involving high temperatures [1]. The mathematical difficulties involved in solving problems in these areas are substantial, since the bases for analyzing a radiative field in an absorbing and emitting medium is the equation of radiative heat transfer which is an integro-differential equation written in terms of the radiative intensity [2]. An exact solution of the equation of transfer may require integrations with respect to time, position, wavelength and solid angle. For most practical problems, these complexities are prohibitive and often the gray medium, the black medium and the steady-state assumptions are used to simplify the problem. The discrete ordinates or SN method is a very popular numerical technique, particularly in its simplest form known as the plane-parallel Disort model by Stamnes [3]. The P-N differential approximation has been applied to one-dimensional atmospheres by Dave and Canosa [4] and also in the two-dimensional spherical harmonics spatial grid (SHSG) code [5]. These two deterministic methods have been combined in the spherical harmonics discrete ordinates method (SHDOM) code by Evans [6], which currently provides the main alternative to Monte Carlo methods for modeling three-dimensional atmospheric radiative transfer.

2. Radiative heat transfer

2.1 Radiative heat transfer equation

In general, the radiative heat transfer equation is given by the following relation:

$$\vec{S}\vec{\nabla}I' = -k_e I' + k_a I_b + \frac{k_s}{4\pi}\int_{4\pi} PI' d\Omega \qquad (1)$$

In this relation, the unit vector $\hat{S}$ is defined as follow

$$\hat{S} = \sin\vartheta\cos\phi\hat{x} + \sin\vartheta\sin\phi\hat{y} + \cos\vartheta\hat{z} \qquad (2)$$

The emission coefficient is given by

$$k_e = k_a + k_s \qquad (3)$$

since

$$k_s = k_e\omega \qquad (4)$$

with the medium albedo ω defined as

$$\omega = k_s / k_e \qquad (5)$$

and then

$$k_a = k_e(1-\omega) \qquad (6)$$

The radiative heat transfer Eq.(1) becomes

$$\vec{S}\vec{\nabla}I' = -k_e I' + k_e(1-\omega)I_b(T) + \\ + \frac{k_e\omega}{4\pi}\int_0^{2\pi}\int_{-1}^{1} P(\mu,\phi,\mu',\phi')I'(\mu',\phi')d\mu' d\phi' \qquad (7)$$

Considering the two dimensional x and Y plane, and assuming $k_e = k$, the previous radiative heat transfer

equation is written in spherical harmonic as follows [5]

$$\mu\frac{\partial I'}{\partial z}+(1-\mu^2)^{1/2}\cos\phi\frac{\partial I'}{\partial x}= \quad (8)$$

$$-k_e I'+\frac{k_e\omega}{4\pi}\int_0^{2\pi}\int_{-1}^{1}P(\mu,\phi,\mu',\phi')I'(\mu',\phi')d\mu'd\phi'+k_e(1-\omega)I_b(T)$$

since the unit vector is now written as

$$\hat{S}=\sin\vartheta\cos\phi\hat{x}+\cos\vartheta\hat{z} \quad (9)$$

2.1 Description of the problem

In this case, the radiative intensity distribution is represented by a series of spherical harmonics given by

$$I'(\vec{r},\Omega)=\sum_{\ell=0}^{\infty}\sum_{m=-\ell}^{\ell}A_\ell^m(\vec{r})Y_\ell^m(\Omega) \quad (10)$$

With the normalized spherical harmonics given by the following relation

$$Y_\ell^m(\Omega)=\left[\frac{2\ell+1}{4\pi}\frac{(l-m)!}{(l+m)!}\right]^{1/2}e^{jm\phi}P_\ell^m(\cos\theta) \quad (11)$$

where

$$P_\ell^m(\mu)=\frac{\left(1-\mu^2\right)^{\frac{m}{2}}}{n!2^\ell}\frac{d^{m+\ell}\left[\left(\mu^2-1\right)^\ell\right]}{d\mu^{\ell+m}} \quad (12)$$

The above relation is an exact representation for the intensity distribution in the limit as ℓ approaches infinity. The approximation occurs when the series is truncated; for this study the first odd spherical harmonic approximation is considered by assuming that

$$A_\ell^m(\vec{r})=0 \text{ for } \ell \succ N \quad (13)$$

The non dimensional moments of intensity are given by

$$I_0(\vec{r})=\int_{\Omega=4\pi}I'(\vec{r},\Omega)d\Omega \quad (14)$$

$$I_{ij\ldots k}(\vec{r})=\int_{\Omega=4\pi}\hat{\ell}_i\hat{\ell}_j\ldots\hat{\ell}_k I'(\vec{r},\Omega)d\Omega \quad (15)$$

The intensity expression is recast in terms of the nondimensional moments of intensity by substituting equation (10) in equations (14) and (15), performing appropriate integrations, and then algebraically solving for the unknown coefficients $A_\ell^m(\vec{r})$ in terms of the moments. The switch from coefficients $A_\ell^m(\vec{r})$ to moments of intensity is made because the first three types of moments have no physical significance. The zeroth order moment is proportional to the radiative energy density and the first moments are the radiative fluxes in the corresponding coordinate direction. The second moment divided by the speed of light comprises the radiative stress and pressure tensor, analogous to the stress tensor in fluid dynamics. The higher order moments have no specific physical significance and are generated by analogy with the first three.

2.2 Two-dimensional radiation in absorbing-emitting medium

A two dimensional heat transfer in a rectangular enclosure where the intervening medium may absorb and emit radiation is considered [2]. The medium:

i) is assumed to have a refractive index of unity
ii) is assumed to be black and has uniform temperature independent properties and
iii) may have internal energy generation. Also, the medium is assumed to be in local thermodynamic equilibrium and, further to be in steady-state condition.

The rectangular enclosure is assumed to be infinite in x_2-coordinate direction. The surfaces are isothermal and may diffusely emit radiative energy. The walls may be specular and (or) diffuse reflectors, through the specular reflectivity is uniform for all incidence angles. For situations where adjacent walls have different emissive powers, the corner values will be assumed to be the arithmetic average of the two wall emissive powers.

The surface emissive powers are non-dimensionalized by the emissive power of surface one, which is assumed to be the highest surface temperature in the enclosure. All other variables are defined in the nomenclature. The medium emissive power and intensity are functions of x_1 and x_3 positions in the rectangular enclosure. The intensity distribution is also dependent on the elevation and the azimuthal angles. Radiative transfer in the x_2-coordinate direction is assumed zero. In addition, it is assumed that the convective and the conductive energy exchange mechanisms are unimportant and can be neglected in this analysis. The governing energy conservation relation thus reduces to

$$\frac{\partial Q_{R1}}{\partial\tau_1}+\frac{\partial Q_{R3}}{\partial\tau_3}=\frac{S}{\tau_H} \quad (16)$$

The radiative transfer is obtained by integration of the radiative intensity (multiplied by the direction cosine) over 4π steradian solid angle.

$$Q_{Ri}(\tau_1,\tau_2)=\int_{\Omega=4\pi}\hat{\ell}_1 I'(\tau_1,\tau_2,\Omega)d\Omega \quad (17)$$

Where $d\Omega=\sin\theta d\theta d\phi$ (18)

The nondimensional radiative intensity is obtained from the equation of radiative transfer, given for an absorbing and emitting medium.

$$\hat{\ell}_1 \frac{\partial I'}{\partial \tau_1} + \frac{\partial I'}{\partial \tau_3} + I' = \frac{B}{\pi} \tag{19}$$

Form the two-dimensional geometry considered, the P-1 approximation for the intensity is given by [2]

$$I'(\tau_1, \tau_2, \theta, \phi) = \frac{1}{4\pi}\left[I_0^{'} + 3I_1^{'}\cos\theta + 3I_3^{'}\sin\theta\sin\phi \right] \tag{20}$$

The equation of transfer is transformed into series of partial differential equations in terms of the moments by multiplying Eq.(19) by appropriate direction cosines and integrating over 4π solid angle as follow.

Integration of Eq.(19) gives

$$\int_{4\pi} \hat{\ell}_1 \frac{\partial I'}{\partial \tau_1} d\Omega + \int_{4\pi} \hat{\ell}_3 \frac{\partial I'}{\partial \tau_3} d\Omega + \int_{4\pi} I' d\Omega = \int_{4\pi} \frac{B}{\pi} d\Omega \tag{21}$$

And according to Eq.(14) we have

$$\frac{\partial I_1}{\partial \tau_1} + \frac{\partial I_3}{\partial \tau_3} + I_0 = 4B \tag{22}$$

Multiplication of Eq.(19) by $\hat{\ell}_1$ and integration give

$$\int_{4\pi} \hat{\ell}_1\hat{\ell}_1 \frac{\partial I'}{\partial \tau_1} d\Omega + \int_{4\pi} \hat{\ell}_1\hat{\ell}_3 \frac{\partial I'}{\partial \tau_3} d\Omega + \int_{4\pi} \hat{\ell}_1 I' d\Omega = \int_{4\pi} \hat{\ell}_1 \frac{B}{\pi} d\Omega \tag{23}$$

And according to Eq.(15) we have

$$\frac{\partial I_{11}}{\partial \tau_1} + \frac{\partial I_{13}}{\partial \tau_3} + I_1 = 0 \tag{24}$$

Multiplication of Eq.(19) by $\hat{\ell}_3$ and integration give

$$\int_{4\pi} \hat{\ell}_3\hat{\ell}_1 \frac{\partial I'}{\partial \tau_1} d\Omega + \int_{4\pi} \hat{\ell}_3\hat{\ell}_3 \frac{\partial I'}{\partial \tau_3} d\Omega + \int_{4\pi} \hat{\ell}_3 I' d\Omega = \int_{4\pi} \hat{\ell}_3 \frac{B}{\pi} d\Omega \tag{25}$$

and according to Eq.(15) we have

$$\frac{\partial I_{13}}{\partial \tau_1} + \frac{\partial I_{33}}{\partial \tau_3} + I_3 = 0 \tag{26}$$

The following equations are then obtained for P-1 approximation

$$\begin{cases} \dfrac{\partial I_1}{\partial \tau_1} + \dfrac{\partial I_3}{\partial \tau_3} = 4B - I_0 & (a) \\ \dfrac{\partial I_{11}}{\partial \tau_1} + \dfrac{\partial I_{13}}{\partial \tau_3} = -I_1 & (b) \\ \dfrac{\partial I_{13}}{\partial \tau_1} + \dfrac{\partial I_{33}}{\partial \tau_3} = -I_3 & (c) \end{cases} \tag{27}$$

Since Q_{Ri} is equivalent to I_i [2], the left hand side of the energy conservation relation written in terms of intensity is the same as the first equation of Eq.(27). This leads to the following

$$\frac{\partial Q_{R1}}{\partial \tau_1} + \frac{\partial Q_{R3}}{\partial \tau_3} = \frac{\partial I_1}{\partial \tau_1} + \frac{\partial I_3}{\partial \tau_3} \tag{28}$$

and consequently

$$\frac{S}{\tau_H} = 4B - I_0 \tag{29}$$

Which leads to the following relation

$$B(\tau_1, \tau_2) = \frac{1}{4}\left(\frac{S}{\tau_H} - I_0 \right) \tag{30}$$

Using the following closure constraints

$$I_{ij} = \frac{1}{3}\delta_{ij} I_0 \tag{31}$$

We have

$$I_{13} = 0,\ I_{11} = \frac{1}{3} I_0 \text{ and } I_{33} = \frac{1}{3} I_0 \tag{32}$$

The Eq.(27) becomes

$$\begin{cases} \dfrac{\partial I_1}{\partial \tau_1} + \dfrac{\partial I_3}{\partial \tau_3} = \dfrac{S}{\tau_H} \\ I_1 = -\dfrac{1}{3}\dfrac{\partial I_0}{\partial \tau_1} \\ I_3 = -\dfrac{1}{3}\dfrac{\partial I_0}{\partial \tau_3} \end{cases} \tag{33}$$

The derivations of the second and third equations of the previous relation lead to

$$\begin{cases} \dfrac{\partial I_1}{\partial \tau_1} = -\dfrac{1}{3}\dfrac{\partial^2 I_0}{\partial \tau_1^2} \\ \dfrac{\partial I_1}{\partial \tau_3} = -\dfrac{1}{3}\dfrac{\partial^2 I_0}{\partial \tau_3^2} \end{cases} \quad (34)$$

Inserting Eq.(27) into Eq.(33a) one obtain

$$\frac{\partial^2 I_0}{\partial \tau_1^2} + \frac{\partial^2 I_0}{\partial \tau_3^2} = -3\frac{S}{\tau_H} \quad (35)$$

since from the definition we have

$$r = \frac{L}{H} = \frac{\tau_L}{\tau_H},\ \eta = \frac{x_1}{H} \text{ and } \chi = \frac{x_3}{H} \quad (36)$$

The differentiation of these relations leads to the following relation

$$\frac{\partial^2 I_0}{\partial \chi^2} + \frac{\tau_L^2}{\tau_H^2}\frac{\partial^2 I_0}{\partial \eta^2} = -3\frac{r\tau_L^2 S}{\tau_L} \quad (37)$$

which can be well written as

$$\frac{\partial^2 I_0}{\partial \chi^2} + r^2\frac{\partial^2 I_0}{\partial \eta^2} = -3r\tau_L S \quad (38)$$

The radiative flux in the x1 direction is given by

$$I_1(\chi,\eta) = -\frac{1}{3}\frac{\partial I_0}{\partial \eta} \quad (39)$$

The radiative flux in the x3 direction is given by

$$I_3(\chi,\eta) = -\frac{1}{3}\frac{\partial I_0}{\partial \chi} \quad (40)$$

2.3 Boundary conditions

The exact boundary conditions are satisfied in an integral sense by utilizing the general Marshak conditions for P-1 approximation as shown in the following relation

$$\int_{\Omega=2\pi} I'(\vec{r},\Omega)Y_\ell^m(\Omega)d\Omega = \int_{\Omega=2\pi} f_w Y_\ell^m(\Omega)d\Omega \ \ (\ell = 1) \quad (41)$$

$$f_w(\vec{r},\Omega) = \varepsilon_i\frac{B_i}{\pi} \quad (42)$$

The normalized spherical harmonics are posed in terms of direction cosines and the integrations are performed for the hemisphere of solid angles over the boundary surface. We obtain the following

$$\begin{cases} I_0(\chi,0) = \dfrac{2}{3}\dfrac{\partial I_0}{\partial \eta}_{\chi,0} + 4B_1 \\ I_0(\chi,1) = -\dfrac{2}{3}\dfrac{\partial I_0}{\partial \eta}_{\chi,1} + 4B_2 \\ I_0(0,\eta) = \dfrac{2}{3}\dfrac{\partial I_0}{\partial \chi}_{0,\eta} + 4B_3 \\ I_0(1,\eta) = -\dfrac{2}{3}\dfrac{\partial I_0}{\partial \chi}_{1,\eta} + 4B_4 \end{cases} \quad (43)$$

2.4 Resolution method

The method used here is the Patankar's method for discretization [7].

$$\frac{\partial}{\partial \chi}\left(K_1\frac{\partial T}{\partial \chi}\right) + \frac{\partial}{\partial \eta}\left(K_2\frac{\partial T}{\partial \eta}\right) + S = 0 \quad (44)$$

Integrating the previous relation from the west point to the east point gives

$$\int_w^e \frac{d}{d\chi}\left(K_1\frac{dI_0}{d\chi}\right)d\chi + \int_w^e \frac{d}{d\eta}\left(K_2\frac{dI_0}{d\eta}\right)d\chi + \int_W^e Sd\chi = 0 \quad (45)$$

Given that the derivative of I_0 is evaluated:

at the east point as

$$\left(\frac{dI_0}{d\chi}\right)_e = \frac{I_{0E} - I_{0P}}{(\delta\chi)_e} \quad (46)$$

at the west point as

$$\left(\frac{dI_0}{d\chi}\right)_W = \frac{I_{0P} - I_{0W}}{(\delta\chi)_W} \quad (47)$$

at the north point as

$$\left(\frac{dI_0}{d\eta}\right)_N = \frac{I_{0N} - I_{0P}}{(\delta\eta)_N} \quad (48)$$

and at the south point as

$$\left(\frac{dI_0}{d\eta}\right)_S = \frac{I_{0P} - I_{0S}}{(\delta\eta)_S} \quad (49)$$

We obtain the following relation

$$K_{1e}\frac{(I_{0E}-I_{0P})}{(\delta\chi)_e}-K_{2W}\frac{(I_{0P}-I_{0W})}{(\delta\chi)_W}+S\Delta\chi=0 \quad (50)$$

Following the same route, we perform the second integration which leads to the relation

$$a_P I_{0P}=a_e I_{0e}+a_W I_{0W}+a_N I_{0N}+a_S I_{0S}+b \quad (51)$$

With

$$a_e=\frac{(K_1)_e}{(\delta\chi)_e}\Delta\eta \quad ; \quad a_W=\frac{(K_1)_W}{(\delta\chi)_W}\Delta\eta$$

$$a_N=\frac{(K_2)_N}{(\delta\chi)_N}\Delta\chi \quad ; \quad a_S=\frac{(K_2)_S}{(\delta\chi)_S}\Delta\chi$$

$$a_P=a_e+a_W+a_N+a_S\,;\; b=3r\tau_L S\Delta\chi\Delta\eta$$

$$K_1=1 \quad \text{and} \quad K_2=r^2 \quad (52)$$

The Eq.(51) is the discretized form of Eq.(38)

3. Results and discussion

For the numerical simulation of Eq.(37), we have considered the following assumptions:

- There is no thermal source S=0
- The aspect ratio is equal to unity r=1
- The nondimensional emissive powers are given by B_1 =1 and B_i =0 (i=2..4)

3.1 Validation of the results

Our results obtained by the P-1 approximation, are compared with those obtained by Larsen (Ratzel III and Howell, 1983) using the Hottel zone code which is the most widely used numerical method for predicting two-dimensional emissive power and heat transfer results in rectangular enclosures.

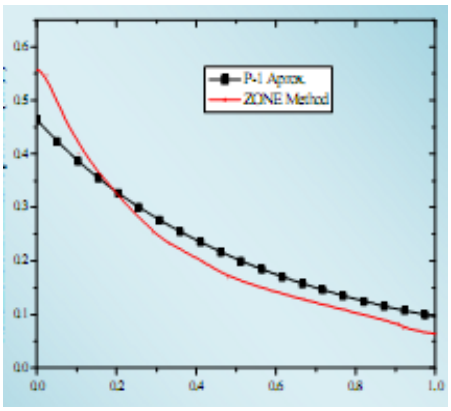

Fig. 1 Comparative P-1 approximation result for nondimensional emissive power $B(\eta)$ versus the normalized position η ($for\ \chi=0.1$).

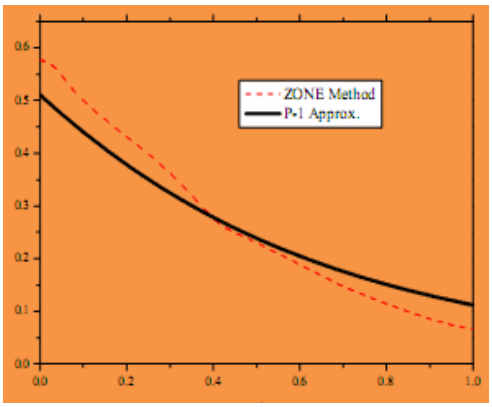

Fig. 2 Comparative P-1 approximation result for nondimensional emissive power $B(\eta)$ versus the normalized position η ($for\ \chi=0.3$).

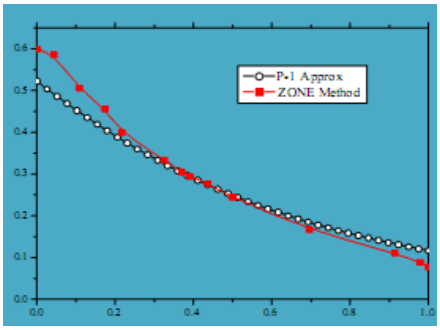

Fig. 3 Comparative P-1 approximation result for nondimensional emissive power $B(\eta)$ versus the normalized position η ($for\ \chi=0.5$).

The above comparative curves allow us to conclude that the P-1 approximation used in this work can be assumed convergent to the results of numerical Hottel zone code for the determination of the emissive powers.

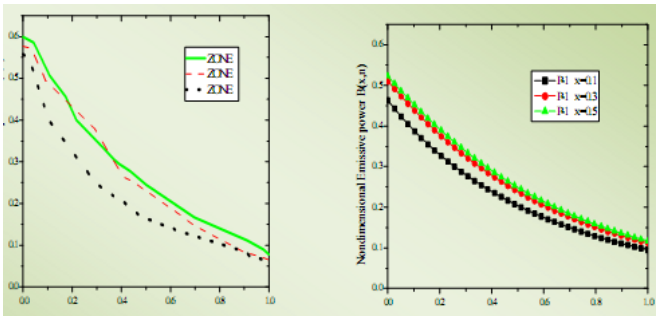

(a) (b)

Fig. 4 Nondimensional emissive power $B(\eta)$ versus the normalized position η (a) Zone code result, (b) P-1 approximation result for $(for\ \chi = 0.1; \chi = 0.3;\ \chi = 0.5)$.

The previous figure allows us to confirm that our P-1 approximation's results and those of Hottel Zone method are almost the same.3.2 Numerical results

3.2.1 Zeroth moment

The zeroth moment solution of the Eq.(38) with boundary conditions Eq.(43) obtained in the previous section is given by the following figure.

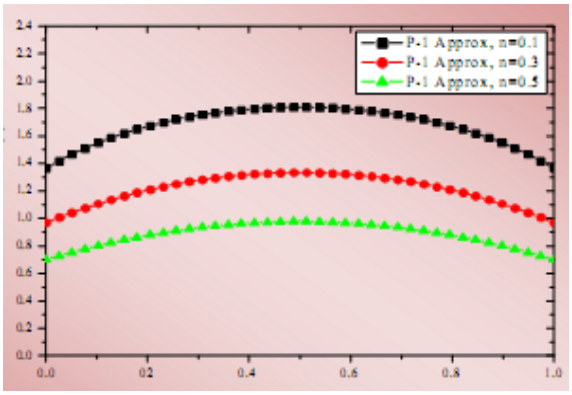

Fig. 5 Distribution of the nondimensional Zeroth moment $I_0(\chi)$ versus the normalized position χ using the P-1 approximation result $(for\ \eta = 0.1; \eta = 0.3;\ \eta = 0.5)$.

We observe from this figure that the Zeroth moment increases (with the x_1 coordinate) till a maximum value before decreasing. It should be noted that the Zeroth moment's and the radiation energy density distribution have the same behavior since the Zeroth moment is proportional to the radiative enrgy density [2].

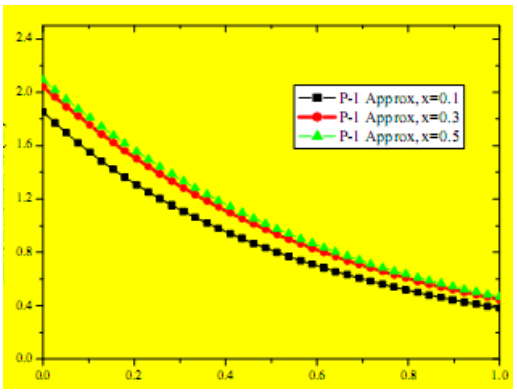

Fig. 6 Distribution of the nondimensional Zeroth moment $I_0(\eta)$ versus the normalized position η using the P-1 approximation result $(for\ \ \chi = 0.1; \chi = 0.3;\ \chi = 0.5)$.

The above curve shows the P-1 approximation distribution of the Zeroth moment (radiation energy density) xhich decreases with the position (x_3 coordinate).

3.2.2 Emissive power

The nondimensional emissive power $B(\eta)$ distributions are given in terms of the nondimensional position η for $\chi = 0.1,\ \chi = 0.3$ and $\chi = 0.5$.

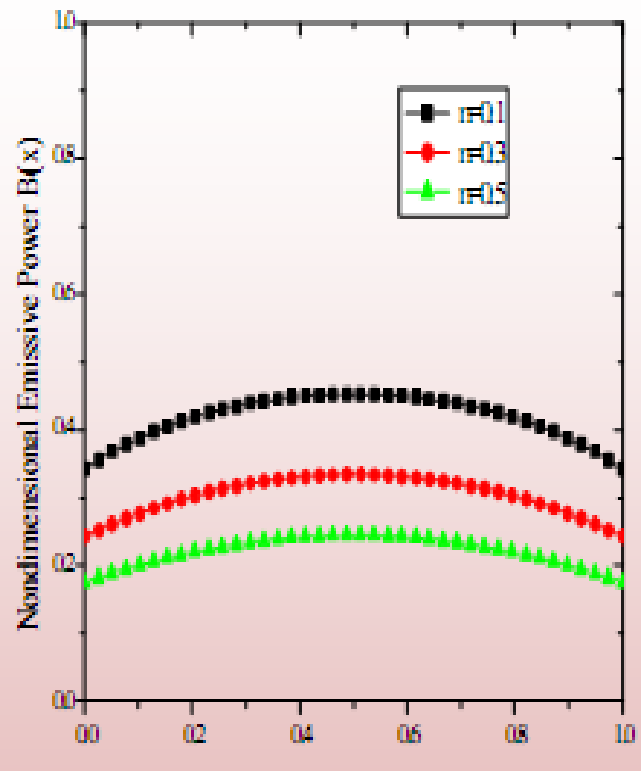

Fig. 7 Distribution of the nondimensional Emissive Power $B(\chi)$ versus the normalized position χ using the P-1 approximation result ($for\ \eta = 0.1; \eta = 0.3; \eta = 0.5$).

3.2.3 Heat transfer rate (Flux)

The following curves show the distribution of heat transfer rate for the P-1 approximation.

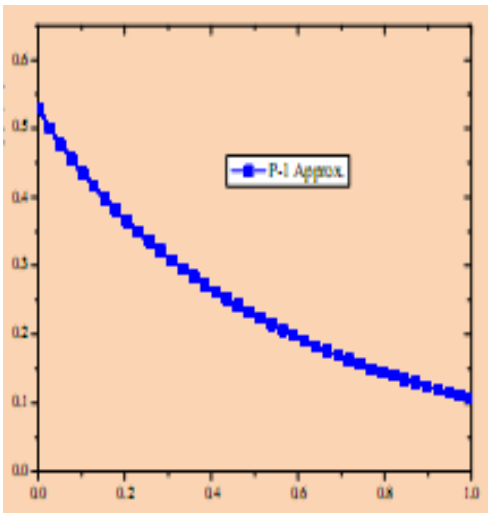

Fig. 8 P-1 approximation result for the nondimensional surface heat transfer rate versus the normalized position η at the left surface $\chi = 0$.

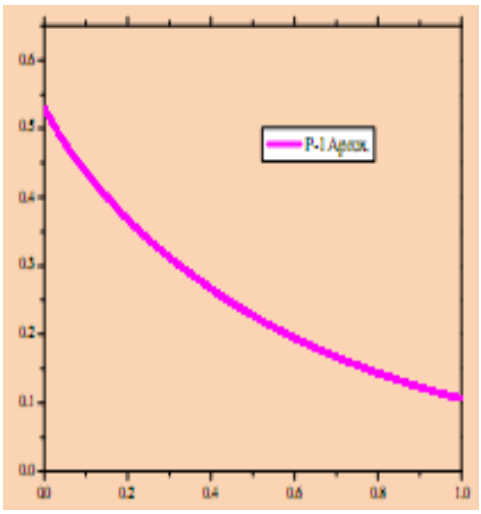

Fig. 9 P-1 approximation result for the nondimensional surface heat transfer rate versus the normalized position η at the right surface $\chi = 1$.

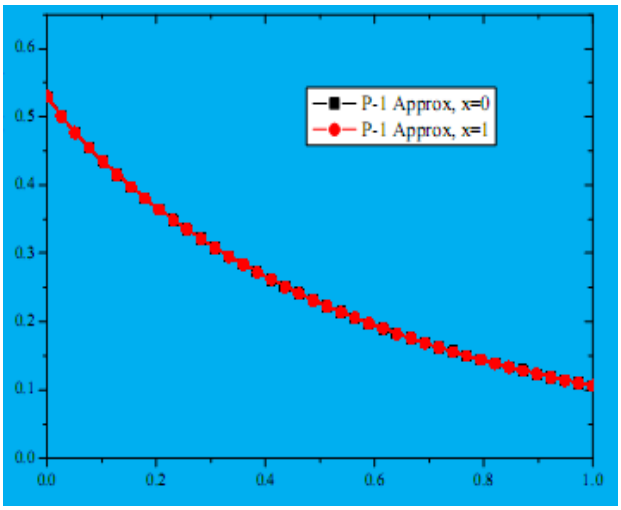

Fig. 10 Comparative P-1 approximation result for the nondimensional surface heat transfer rate versus the normalized position η at both the left right surfaces.

The previous figure shows that the results for the nondimensional left and right surfaces heat transfer rates coincide.

4. Conclusions

In this work, we have presented the radiative heat transfer equation and described the problem of a two-dimensional combustion chamber. The solution of the radiative heat transfer equation was obtained using the P-1 approximation followed by the Patankar's method. We also compared the emissive power's curves with those of the literature on one hand and drawn many other curves describing the evolution of some physical quantities in the combustion chamber (rectangular enclosure) on the other hand. The results have been convincing although we limited our study on the P-1 approximation.

References

[1] M. SANDIP, "A new numerical procedure for coupling radiative in participating media with other modes of heat transfer", Journal of heat transfer, vol.127,2005,pp.1037-1045.

[2] A.C RATZEL, J.R HOWELL, "Two-dimensional radiation in absorbing-emitting media using the P-N approximation", Journal of heat transfer, Vol.105, 1983, pp.333-340.

[3] K. STAMNES etal., "Numerical stable algorithm for discrete-ordinate method radiative transfer in multiple scattering and emitting layered media" Appl. Opt. 27, 1998, pp.252-2509.

[4] J.V DAVE, J. CANOSA, "A direct solution of the radiative transfer equation : Application to atmospheric models with arbitrary vertical nonhomogeneities", J. Atmos. Sci. 31, 1974, pp. 1089-1101.

[5] K.F EVANS, "The spherical harmonics discrete ordinate method for three-dimensional atmospheric radiative transfer", J. Atmos. Sci. 50, 1993, pp. 3111-3124.

[6] K.F EVANS, "Two-dimensional radiative transfer in cloudy atmosphere: the spherical harmonics spatial grid method", J. Atmos. Sci. 55, 1998, pp. 429-446.

[7] PATANKAR, "Numerical heat transfer and heat flow", Series in computational methods in mechanics and thermal sciences 205p.